Vietnam Journal of Earth Sciences, 45(1), 98-110, https://doi.org/10.15625/2615-9783/17924

Vietnam Journal of Earth Sciences
https://vjs.ac.vn/index.php/jse

Numerical modelling of slope stabilization with xathan gum-treated soil

Tran Thi Phuong An[1*], Chang Ilhan[2], Tran Thanh Nhan[1], Cho Gye-Chun[3]

[1]*Department of Hydrogeological and Geotechnical Engineering, University of Sciences, Hue University, 77 Nguyen Hue, Hue 49000, Vietnam*
[2]*Department of Civil System Engineering, Ajou University, 206 Worldcup-ro, Yeongtong-gu, Suwon 16499, Republic of Korea*
[3]*Department of Civil Engineering, Korea Advanced Institute for Science and Technology, 291 Daehak-ro, Yuseong-gu, Daejeon 34141, Republic of Korea*

Received 25 June 2022; Received in revised form 02 November 2022; Accepted 02 December 2022

ABSTRACT

Biopolymer soil treatment has been introduced as the latest technological innovation in soil stabilization and improvement. Biopolymers with agar, guar, xanthan, casein, gellan and sodium alginate have been commonly studied to improve strength, reduce hydraulic conductivity and prevent erosion of highly permeable soil materials. Among those, xanthan gum is introduced to perform better in terms of lowering permeability. In this study, the effect of xanthan gum on slope stability under rainfall was evaluated via a 2D finite-difference program (FLAC) considering the wetting behavior of xanthan gum-treated soil. In order to obtain input parameters for numerical modelling, wetting soil-water characteristic tests, permeability tests, and direct shear tests were conducted on xanthan gum-treated soils. The numerical results support the application of biopolymers to soil erosion control during rainfall, mainly due to the significant decrease in the infiltration of xanthan gum-treated soil.

Keywords: xanthan gum, wetting soil-water characteristics, slope stability, rainfall, matric suction, FLAC2D.

1. Introduction

The past decades have witnessed a significantly positive effect of biopolymers on geotechnical properties of soil such as soil strengthening (Chang and Cho, 2019; Chang et al., 2015c; Zhang et al., 2022), water retention improvement (Bhardwaj et al. 2007; Tran et al. 2019; Wang et al., 2023), hydraulic conductivity reduction (Bhardwaj et al., 2007; Chang et al., 2016), and soil erosion prevention (Ko and Kang 2020). Furthermore, biopolymers are recognized as a feasible alternative to conventional chemical polymers because of their low environmental impact, non-toxicity, and non-secondary pollution (Aminpour and O'Kelly, 2015). Using biopolymers can also cut back on the CO_2 emissions from cement which are the source of approximately 5% of global greenhouse gases (Hendriks et al., 1998).

It is known that the hydrophilic structure of biopolymers renders them capable of holding large amounts of water. Therefore, incorporating a biopolymer within soils shows remarkable performance in filling the soil pores by suddenly absorbing infiltrated water and forming viscous hydrogels. In other words, the existence of biopolymer strongly affects the

*Corresponding author, Email: ttphuongan@hueuni.edu.vn

wetting soil-water characteristic curves (SWCCs), which has not been paid serious attention in research on biopolymer-treated soil. In geotechnical and geo-environmental engineering practice, the SWCCs express a constitutive relationship between the water content and suction within the soil (Fredlund et al., 2012). This work focuses on wetting SWCCs, which can provide the parameters for numerical modeling of the seepage flow through unsaturated soil.

The study uses numerical modeling to assess slope stabilization with biopolymer-treated soil. Therefore, xanthan gum biopolymer, which offers excellent performance in reducing permeability among common bio-based biopolymers (Bouazza et al., 2009), was used to treat jumunjin - kaolinite soil mixture. To obtain the wetting SWCCs, a capillary rise open tube was used to measure the wetting SWCC of xanthan gum-treated soil. The SWCC parameters were then obtained and used as input parameters for slope stability modeling with FLAC2D software. Furthermore, the soils' saturated permeability and shear strength parameters (i.e., cohesion and friction angle) were tested for numerical modeling. Consequently, the experimental and numerical modeling results allow observing the effects of the water absorption and holding ability of xanthan gum on the upward movement of water within the soil, the wetting SWCCs, and the factor of safety (*FoS*) of a slope. This study can provide evidence of practical applicability in the geotechnical engineering of xanthan gum biopolymers.

2. Materials and Methods

2.1. Materials

2.1.1. Xanthan gum biopolymer

Xanthan gum (hereafter, XG) is an anionic water-soluble exopolysaccharide synthesized by the *Xanthomonas campestris* bacterium. XG is widely used as an emulsifier, a suspension stabilizer, a flocculant, and a thickening agent in various industrial applications (Chang et al., 2015a; Palaniraj and Jayaraman, 2011). In economic terms, XG is an economically feasible microbial polysaccharide in the global biopolymer market (Mayer et al., 2010). This study used sterilized and purified XG (CAS No.11138-66-2; Sigma Aldrich) for laboratory tests.

2.1.2. Sand (Jumunjin sand)

Jumunjin sand, a standard sand material in Korea with a specific gravity (Gs) of 2.65 (Chang and Cho, 2019; Chang et al., 2016), is classified as a poorly graded sand with D_{50} = 0.43 mm. Its uniformity coefficient (C_u) and coefficient of gradation (C_c) are 1.39 and 0.76, respectively.

2.1.3. Kaolinite

Kaolinite is the most common and less-swelling clay mineral (Osacky et al., 2015). This study used Bintang kaolinite (Belitung Island, Indonesia). The basic properties of clays are shown in Table 1.

Table 1. Basic properties of kaolinite

Properties			Values
Specific gravity	G_s	-	2.65
Liquid limit	LL	%	59
Plastic limit	PL	%	25
Average size	D_{50}	μm	44
Specific surface area	S	m^2/g	22

2.1.4. Xanthan gum - soil mixture preparation

The dry kaolinite was mixed with dry jumunjin sand with a ratio of clay to sand at 2:8 (S8K2). This ratio was chosen randomly, and a different ratio will be conducted shortly. The soil mixture was mixed with 0.0% (untreated) and 0.5% XG concerning the mass of dry soil. XG solution was prepared by dissolving pure XG powder in deionized water at room temperature (20°C). XG solution was mixed with dry soil at an initial water content equivalent to 10% of the mass of the soil.

2.2. Experimental methods

2.2.1. Wetting SWCCs

A capillary rise tube with a 10 cm diameter and a 50 cm height (Yang et al., 2004) was used (Fig. 1). Thoroughly mixed XG-soil mixture was dried in an oven at 30°C for 30 days before conducting the wetting test. The dried XG-soil mixtures were compacted into the tube at a target dry density of 1.55 (g/cm^3) and placed in a water tray. The top of the tube was sealed with parafilm to prevent evaporation from the soil surface. Water was poured into the tray up to a height of 1.0 cm and maintained during the test. The water in the tray started to move into the soil column. Once the capillary water in the tube reached equilibrium, the 50 cm height soil column was divided into several segments to determine the variation in the gravimetric water content along the soil column.

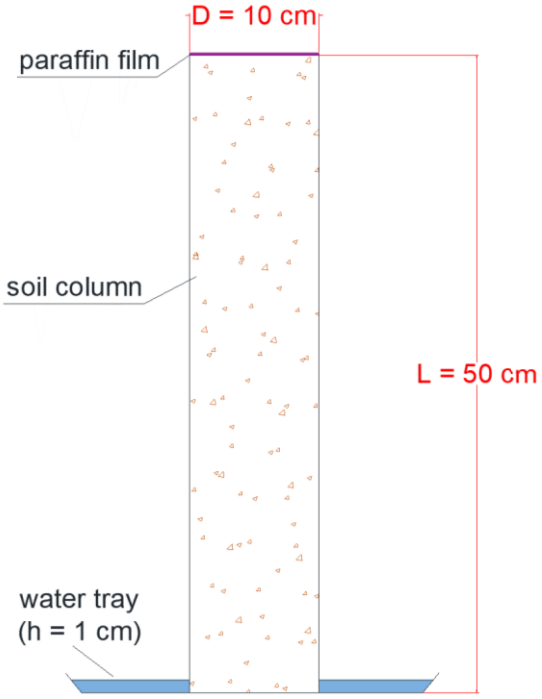

Figure 1. Capillary column test diagram

The matric suction (u_a–u_w) inside the soil tube was calculated as: ρ_f (the density of fluid) × g (the acceleration due to gravity: 9.81 m/s^2) × H (the height of the water inside the soil column, regarded as the negative pore-water pressure head in soil, in m). A fluid density of 1.0 g/cm^3 was used in this study.

2.2.2. Direct shear test

A direct shear testing device (Humboldt HM-2560A) performed direct shear tests. XG-soil mixture at initial state was molded in a shear ring having a 6 cm inner diameter and 2.5 cm height and oven-dried at 30°C until reaching a constant weight. Then the specimen was placed in a circular shear box with porous stones above and beneath. The confining pressures of 50, 100, and 200 kPa were applied via a pneumatic actuator for 24 h to ensure no further vertical displacement before the horizontal shear displacement test. Horizontal shear displacement was applied at a rate of 0.01 mm/min (ASTM, 2011). The tests were conducted at room temperature (20±1°C).

2.2.3. Hydraulic conductivity test

XG-soil mixtures were poured into an EVP mold with an inner diameter of 5 cm and a height of 10 cm before being dried in the oven. Permeability tests were performed using a flexible wall permeameter at room temperature (20±1°C) while the inlet and outlet flows were controlled and maintained using a pressure panel. A head difference of 150 mm was applied to saturate the specimen thoroughly, and confining pressure of 30 kPa was applied. When the Skempton B-values of the samples exceeded 95%, the samples were then considered fully saturated. After saturation, falling-head permeability tests were performed according to ASTM standard D5084 (ASTM 2010).

2.3. Analytical methods

2.3.1. Soil water characteristic curve

The Van Genuchten formula (Van

Genuchten 1980) is commonly used for SWCC and seepage models for various soils. The volumetric water content (θ_w) of soil is expressed as:

$$\theta_w = \theta_r + \frac{(\theta_s - \theta_r)}{\left[1+(\psi/\alpha)^n\right]^m} \quad (1)$$

where θ_s is the saturated volumetric water content; θ_r is the residual volumetric water content; ψ is the soil suction (kPa); α is a soil parameter related to the air entry value (*AEV*); n is a soil parameter associated with the rate of water extraction from the soil; and m is a soil parameter related to θ_r and m, which can be calculated using $m = 1 - (1/n)$ (Mualem 1976a, 1976b). In this study, Eq. (1) was used to obtain the wetting SWCC parameters of the XG-treated soils using a nonlinear fitting program (Seki 2007).

2.3.2. Analytical method of calculating seepage

The yield criterion of the unsaturated soil is as follows (Fredlund et al. 1978).

$$\tau_{\max} = (\sigma - u_a)\tan\phi' + \frac{S_w - S_r}{1 - S_r}(u_a - u_w)\tan\phi' + c' \quad (2)$$

where τ_{max} is the material shear strength, ϕ' is the effective friction angle of the soil, c' is the effective cohesion of the soil, S_w is the degree of saturation, and S_r is the residual saturation. Moreover, the shear strength parameters, cohesion (c^{trial}), and friction angle (ϕ^{trial}) are defined as follows.

$$c^{trial} = \frac{1}{F^{trial}} \cdot c' \quad (3)$$

$$\phi^{trial} = \arctan\left(\frac{1}{F^{trial}} \cdot \tan\phi'\right) \quad (4)$$

where F^{trial} is the trial factor of safety. The initial F^{trial} value is set sufficiently low to ensure that the system is stable. The value is incrementally increased until failure. The critical factor at which failure occurs is taken to be the factor of safety.

A set of closed-formed equations is used to simulate the hydraulic characteristics of unsaturated soils (ITASCA 2011):

$$S_e = \frac{S_w - S_r}{1 - S_r} = \left[\frac{1}{1+(\alpha \cdot \psi)^n}\right]^m \quad (5)$$

$$\left|K(\theta)\right| = K_s \cdot K_r = K_s \cdot S_e^{1/2}\left[1-\left(1-S_e^{1/m}\right)^m\right]^2 \quad (6)$$

where S_e is the effective saturation, $m = 1 - 1/n$, $n > 1$; $K(\theta)$ is the permeability of the soil, and K_s and K_r are the saturated and relative permeabilities, respectively.

2.3.3. Numerical analysis

A numerical simulation was developed to evaluate the stability of a slope with and without biosoil treatment during a rainstorm. To simulate the matric suction distribution in an unsaturated slope, a two-phase flow was used in the numerical modeling. In this study, there is no horizontal displacement along the bottom mesh boundary of the slope. As the rainfall intensities are applied along the slope (i.e., rainwater-infiltrating boundary), the flow modeling with FLAC is done in parallel with the mechanical modeling. At the rainfall-infiltrating boundary, the pore air pressure is ambient (i.e., zero). Fig. 2 shows the simulation's overall algorithm to assess this study's main point of interest.

The geometry of a real slope (N57°46'19.6'', E127°16'46.4''; Namyangju, Republic of Korea) was considered for numerical simulation. The site slope (39 m in height, 22° in average inclination) was reconstructed to contain the S8K2 soil along its surface in this study. For precipitation simulation, a heavy downpour (intensity = 1.125 m/h) condition, which was reported to have caused severe debris flow in 2011 (Mt. Umyeon, Seoul, Republic of Korea, on 27 July 2011) (Jeong et al., 2015) was employed. The biosoil treatment method was applied along the weakest area for a depth of 0.06 m.

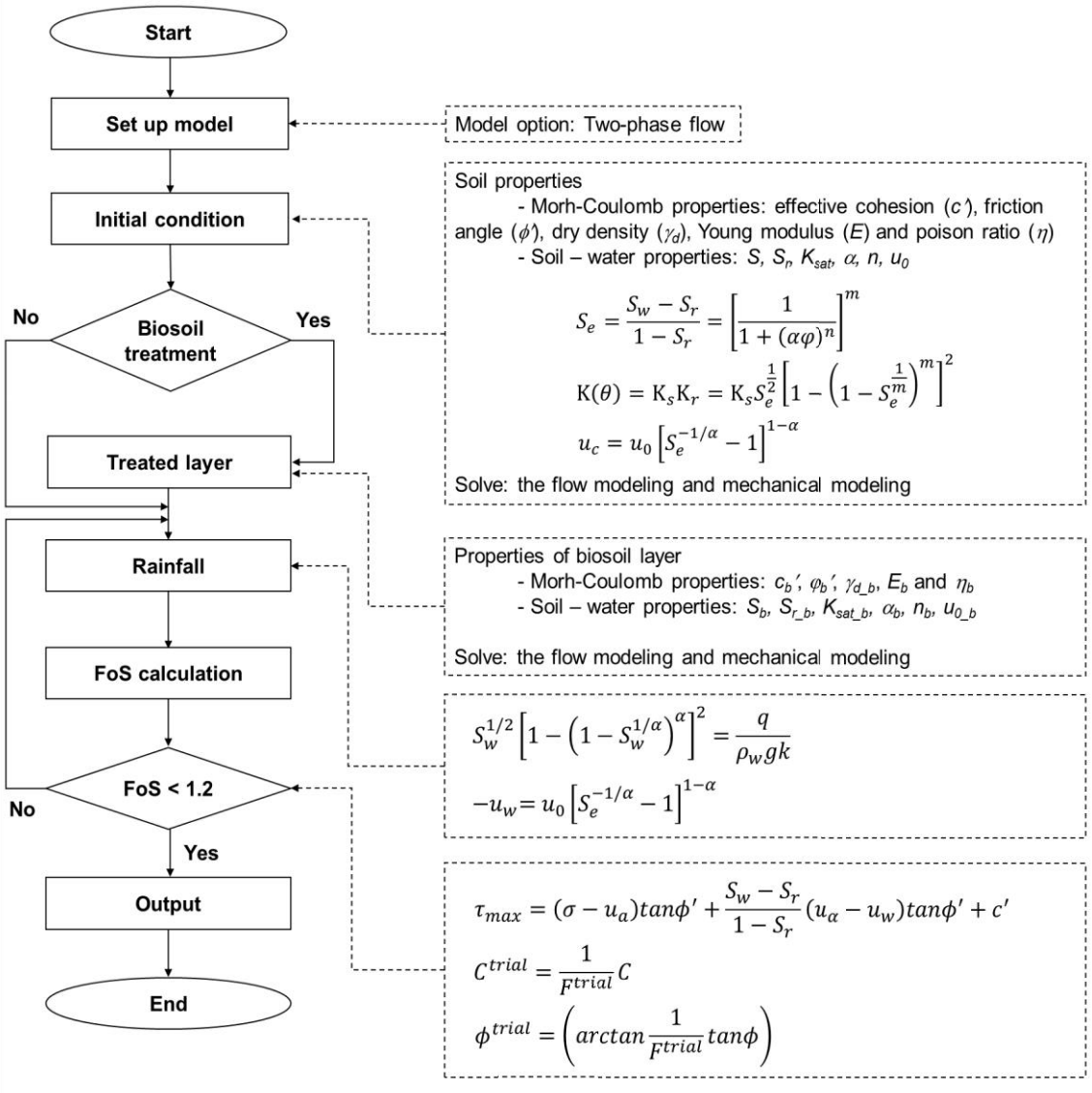

Figure 2. Algorithm of numerical analysis o slope stability with biosoil treatment using rainfall

4. Results

4.1. Effect of xanthan gum on geotechnical engineering properties of soils

4.1.1. Wetting soil-water characteristics

Figure 3 and Table 2 present the wetting SWCCs and relevant parameters of the untreated and 0.5% XG-treated S8K2 soils. The saturated volumetric water content (θ_s) of the treated soil (θ_s = 0.4) is higher than that of the untreated soil (θ_s = 0.28) because of the high water-holding capacity of the XG hydrogels (Bhardwaj et al. 2007; Hatakeyama and Hatakeyama, 1998; Zhang et al., 2017). At a certain suction level, XG helped increase the pore-clogging and surface tension, significantly reducing the water suction. The difference becomes negligible when the matric suction is ≥ 5 kPa. The volumetric water content (θ_w) values at 5 kPa are 0.136

and 0.122 for the untreated and 0.5% XG-treated S8K2 soil, respectively.

The *n* value of the XG-treated soil (2.27) is significantly higher than that of the untreated soil (1.81), whereas the difference in the *m* values is less. The *n* parameters, which express the water loss rate of the soil, do not follow the sigmoid relationship with XG content which was found from the drying SWCCs for the XG-treated sand-10% kaolinite mixture (Tran et al., 2020). In this study, the higher *n* value for the treated soil is due to the bio-clogging-induced water content gap, instead of a high water loss rate, between soil suctions at 1 kPa and 3 kPa.

The WEV is the point where the water starts entering the soil. The untreated soil creates a higher suction (i.e., 8.5 kPa) to prevent the soil from being wetted (Wang et al., 2000). When the XG is added to the soil, its water absorption quickly caused the soil to wet at the beginning of the wetting test; therefore, the WEV obtained was 7.0 kPa (Fig. 3, Table 2).

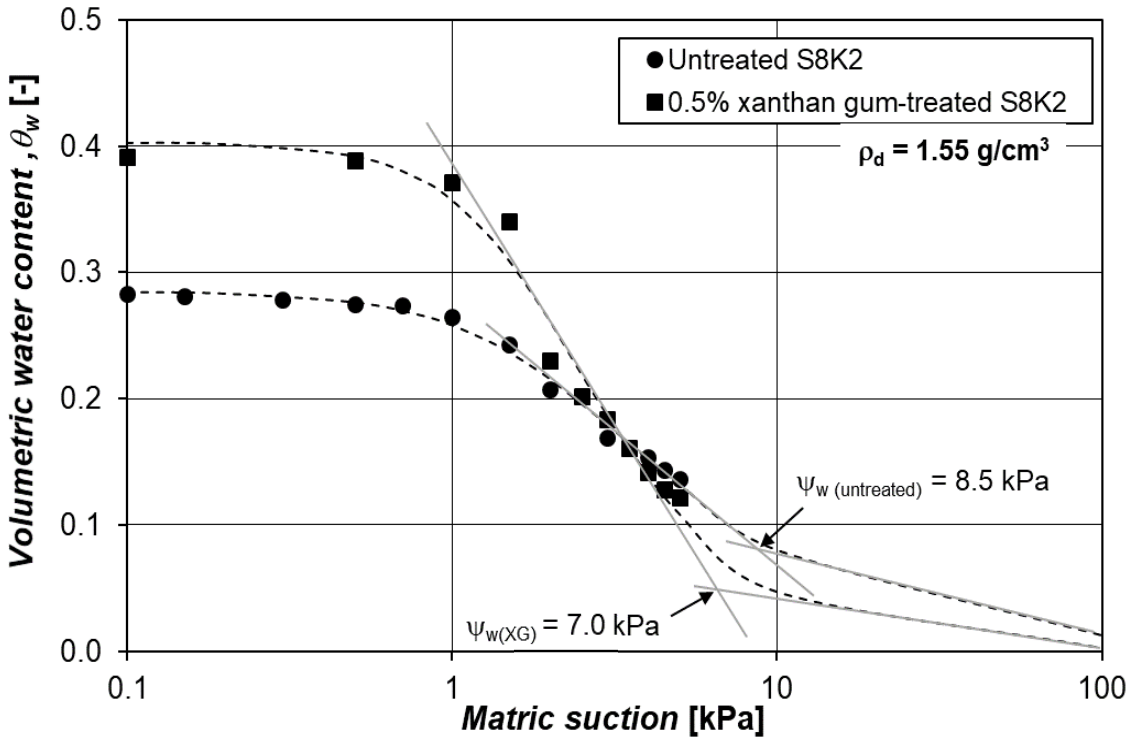

Figure 3. Wetting soil-water characteristic curves of the untreated and 0.5% xanthan gum-treated S8K2 soil

Table 2. SWCC parameters of untreated S8K2 and XG-treated S8K2

Van Genuchten parameters		20% kaolinite-sand mixture	
		Untreated	Treated
θ_s		0.28	0.40
θ_r		0	0
α	[kPa $^{-1}$]	0.46	0.54
n		1.81	2.27
m		0.45	0.55
WEV	[kPa]	8.50	7.00

The results demonstrate the significant effect of XG on the water holding capacity of the soil (i.e., θ_s or θ_w) at suction levels lower than 5 kPa. The SWCCs' parameters were summarized in Table 2.

4.1.2. Hydraulic conductivity

The hydraulic conductivity of the XG-treated soil increased from the untreated

condition (4.519×10^{-7} m/s) to 0.5% xanthan gum content (1.573×10^{-9} m/s). For untreated soil, pore-clogging induced by kaolinite played the primary role in holding water and controlling water flow within soil (Fig. 4a). As the soil was treated with XG, kaolinite-XG matrix was established and enhanced the water-holding ability and resistance to upward water flow in the soil (Fig. 4b). The decrease in the hydraulic conductivity of the soil is due to XG-induced pore-clogging (Bouazza et al., 2009; Chang et al., 2016), which exceeded two orders of magnitude compared to the untreated condition in this study.

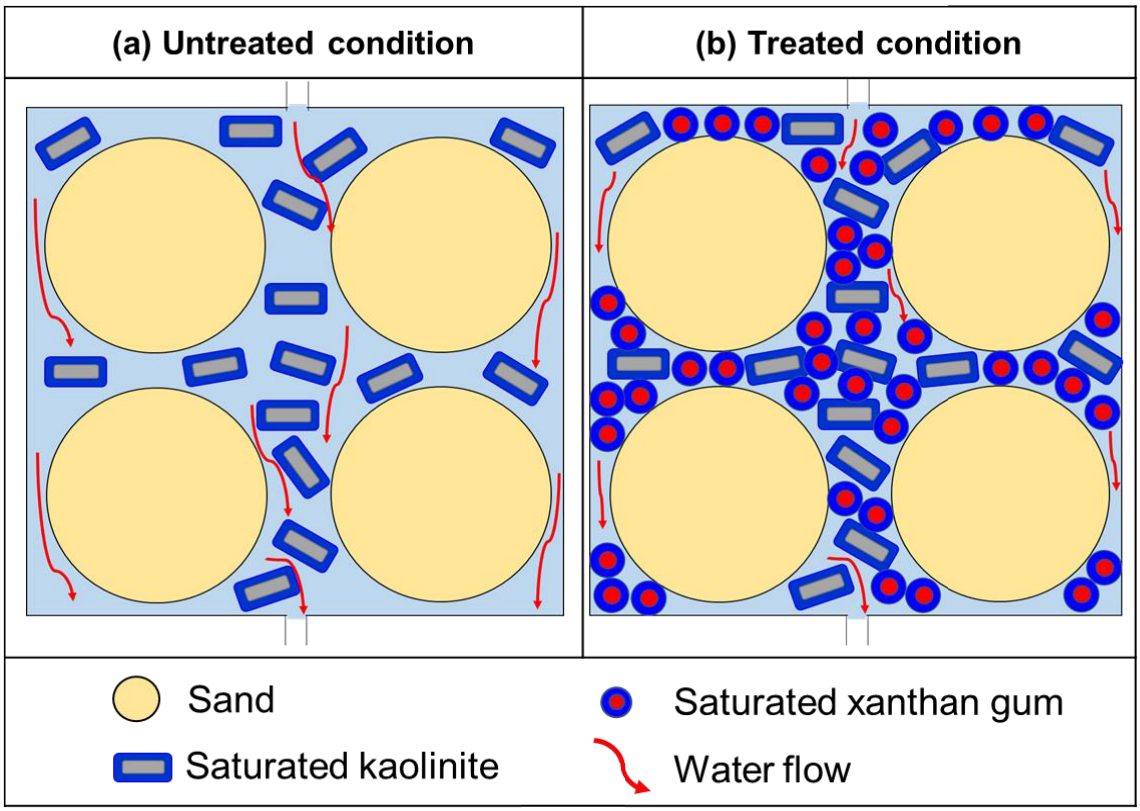

Figure 4. Pore clogging effect occurring in untreated and treated soil during hydraulic conductivity test

4.1.3. Shear strength properties

Horizontal displacement - direct shear stress behaviors of untreated and XG-treated at dried conditions are presented in Fig. 5. The peak shear strength of XG-treated soil is significantly higher than the untreated one, regardless of confinement pressures. The shear strength improvement was because dehydrated XG acted as bridges that enhanced the inter-particle contacts between kaolinite and sand particles. Furthermore, XG also served as filler material for soil, reducing the void spaces. The high viscosity of XG, after the dehydration process, increases the cohesion of soil significantly from 25 kPa (untreated condition) up to 176 kPa (treated condition), while a light enhancement in friction angle is obtained. The changes in peak strength with confinement pressures and peak strength parameters are summarized in Table 3.

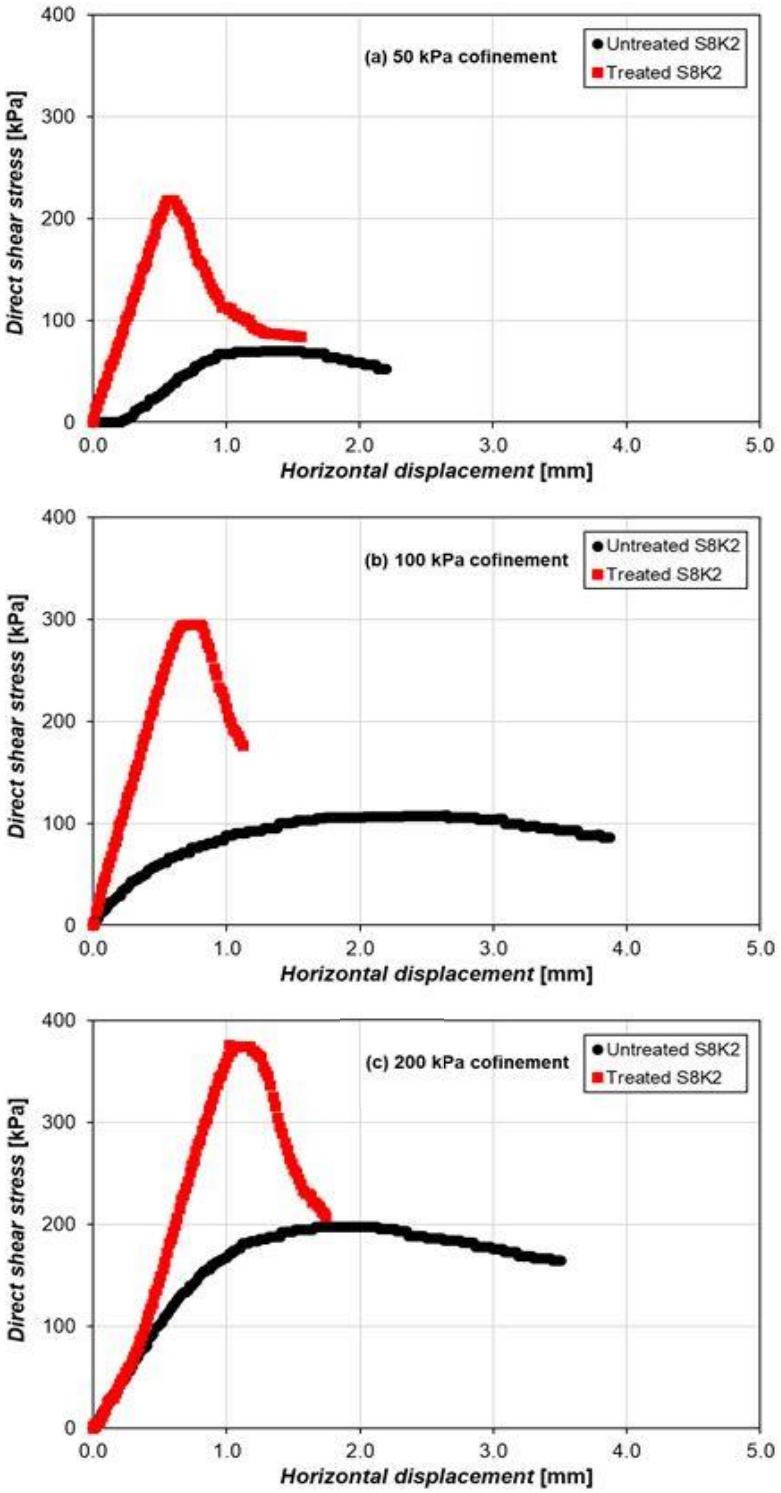

Figure 5. Stress-strain relationship of xanthan gum-treated S8K2 at confinement pressures of (a) 50 kPa, (b) 100 kPa and (c) 200 kPa

Table 3. Shear strength parameters for untreated S8K2 and XG-treated S8K2

Confine pressures	[kPa]	Untreated soil	Treated soil
		Shear stress peak	
50		70.24	218.21
100		107.93	295.38
200		197.92	376.49
Cohesion	[kPa]	25	176
Friction angel	°	49.5	57.4

4.2. Effect of xanthan gum treatment on shallow slope stability

Table 4 summarizes the basic geotechnical engineering properties and soil-water characteristics of the soils. The effective cohesion values were taken as zero to avoid overestimating the factor of safety (*FS*), as the failure surface is shallow (Fell, 2005).

Table 4. Input parameters for FLAC simulation

Parameters		Values		Unit
		Untreated S8K2	XG-treated S8K2[1)]	
Dry density		1.55	1.55	g/cm^3
Cohesion (c')		0	0	kPa
Friction angle (ϕ')		49.5	57.4	°
Saturation		0.5	0.5	
Residual volumetric water content (θ_r)		0	0	
Van Genuchten parameters	α	0.46	0.54	kPa^{-1}
	m	0.45	0.55	
Saturated permeability of soil (K_{sat})		4.519×10^{-7}	1.573×10^{-9}	m/s

[1)] 0.5% xanthan gum (xanthan gum to soil ratio, in mass)

Figure 6 shows the geometry of the slope. Its initial FS. Using FLAC2D, the weakest area along the slope surface was assessed to be the area beginning from the 38th point from the left boundary and extending downward along the slope with a length of 23 m (Fig. 6a). The predicted failure area of the slope was simulated to be treated with the 0.5% XG-treated S8K2 soil with a thickness of 6 cm along the 38-m length, which appropriately forms a biopolymer-soil layer over the weakest area (Fig. 6b). To characterize the treated area, the soil properties of the weakest area are replaced by those of the XG-treated soil listed in Table 4. The change in the pore water pressure with depth in the weakest area (A-A′) (Fig. 6b) was estimated for the treated and untreated slopes.

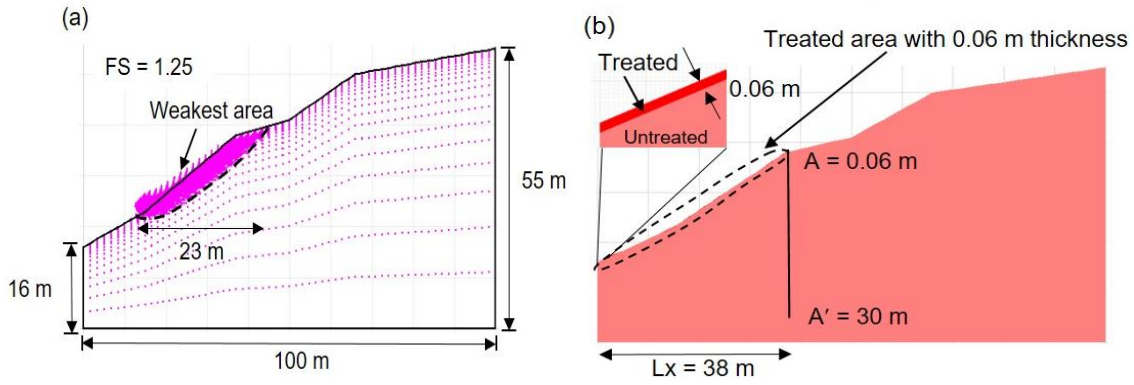

Figure 6. Target slope for numerical verification. (a) Overall geometry and weakest area of the slope. (b) Xanthan gum treatment simulation (0.06-m-thickness from the toe up to the entire weakest area)

Figure 7 shows the negative pore pressure (i.e., the matric suction) distribution along cross-sections A-A' before and after rainfall. At a depth of 0.06 m, the negative pore pressure of the 0.5% XG-treated slope (5.09 × 10^3 kPa) is slightly lower than that of the untreated slope (5.30 × 10^3 kPa) (Figs. 7a and b) before rainfall. The slight increase of the matric suction has a negligible effect on the shear strength (Eq. 2) and the corresponding FS value. However, after 40 hours of rainfall, the negative pore-water pressure of the XG-treated slope is higher than that of the untreated slope (Figs. 7a, b) because of the XG treatment on the surface of the weakest area; the treatment helped retain the surface infiltration into the ground by lowering the hydraulic conductivity. Thus, the XG treatment allows the entire slope to remain safe for longer than the untreated slope under continuous heavy rainfall (Fig. 8). The untreated slope failed after 40 hours under continuous rainfall. In contrast, the slope treated with the 0.5% XG-treated soil on its weakest area surface (for a depth of 0.06 m) remained safe for up to 480 hours. Therefore, a small amount of XG biopolymer (even for a shallow depth of 0.06 m) helps to enhance slope stability against heavy rainfall.

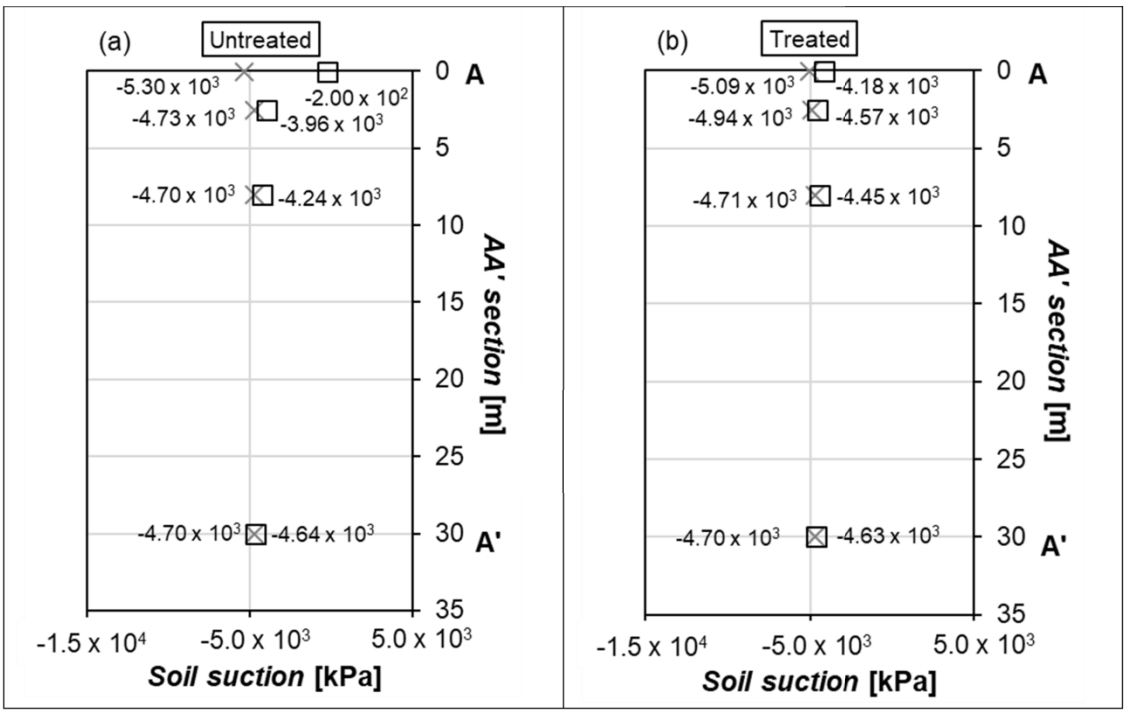

Figure 7. The pore pressure distribution along section AA′ before (×) and after 40-hours (B) of downpour simulation. (a) Untreated slope. (b) 0.5% xanthan gum-treated slope

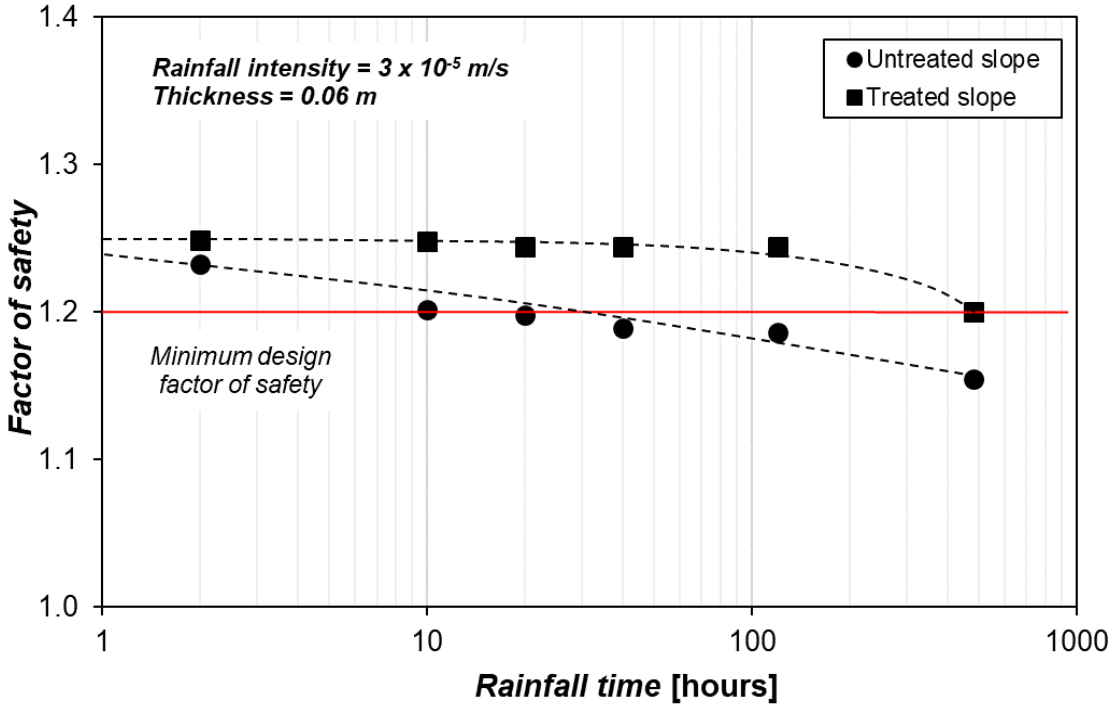

Figure 8. Variation of factor of safety against slope failure under continuous rainfall simulation

5. Discussion: Significance of the wetting SWCC of biopolymer-treated soil

As mentioned above, the XG-treated soils show a distinctive absorption behavior compared to the untreated soils. Specifically, the XG-treated soils show promising potential for preventing immediate infiltration. This study provides an example of utilizing the wetting behavior of the XG-treated soils for slope stability against severe rainfall. In fact, the water-entry suction value of the XG-treated soil ($\psi_{w(XG)}$ = 7.0 kPa) is lower than that of the untreated soil ($\psi_{w(untreated)}$ = 8.5 kPa) (Fig. 3, Table 2). If water entry is the only trigger, the XG treatment should be more vulnerable to slope stability. However, although biopolymers quickly absorb water, the subsequent hydrogel swelling becomes the dominant factor for the behaviour of the entire soil area because of the significant reduction in the soil's hydraulic conductivity (and infiltration). Note that the trend in the wetting SWCC shown in this example is for the 0.5% XG-treated S8K2 soil. Different types of biopolymers at different contents will exhibit different wetting behaviors, particularly in water-entry values. Therefore, the overturning trend in the biopolymer-treated to untreated soil would not occur.

The wetting SWCC, including the capillary conductivity results, provides evidence of biopolymers' applicability to slope treatment. With the high water-holding capacity, the XG biopolymer can easily and effectively perform the roles of restraint, interception, retardation, infiltration, and transpiration as a water barrier liner, as required in ecosystem engineering. A significant advantage of biopolymers over another bio-soil treatments, such as microbiologically induced calcite precipitation, is that the former can be applied to slope surfaces with various soil types. The positive effect of biopolymers on vegetation growth (Chang et al., 2015c; El-Rehim et al.,

2004; Tran et al., 2019) is another advantage of biopolymer slope treatment.

Owing to the valuable properties of biopolymers with respect to water (i.e., high absorption and holding capacity), more attention should be paid to SWCCs of biopolymer-treated soils. This study would be useful to solve problems regarding the performance of biopolymers in geotechnical engineering applications such as slope treatment, water barriers, water storage, and liners in landfills.

6. Conclusions

To assess the effects of XG on the shallow slope stability, laboratory tests (i.e., soil-water characteristics, shear strength properties, and hydraulic conductivity) were conducted on XG-treated sand-20% kaolinite mixture. The experimental results obtained were input parameters for the developed rainfall-induced slope failure analysis. Two main findings of this study are shown as follows,

As an environmentally friendly biopolymer used for soil treatment. The dehydrated XG-treated soil showed relatively high strengthening even at low content (0.5%). The shear strength changes from 25 kPa (untreated condition) up to 176 kPa (treated condition).

The XG hydrogel enhanced water absorption and water holding capacity, which induced the bio-clogging effect and controlled water's upward and downward movement within the soil. The hydraulic conductivity of soil used in this study decreases two order magnitude from 4.519×10^{-7} m/s to 1.573×10^{-9} m/s as treated by 0.5% XG.

The controlling ability of XG for water movement significantly affected the change of matric suction (negative pore water) distributed into the soil during rainfall. In turn, the stability of the slope remained for a longer time of rainfall. As the weakest area is covered by XG-treated soil, the slope remains stable for up to 480 hours.

Acknowledgments

The first and third authors acknowledge the support of Vietnam National Foundation for Science and Technology Development (NAFOSTED) under Grant Number 105.08-2018.01 and Hue University under the Core Research Program Grant No. NCM.DHH.2018.03.

References

Aminpour M., O'Kelly B.C., 2015. Applications of biopolymers in dam construction and operation activities. In Proceedings of the 2nd International Dam World Conference, Lisbon, Portugal. Laboratório Nacional de Engenharia Civil, Lisbon, Portugal, 937-946.

ASTM, 2010. Standard test methods for measurement of hydraulic conductivity of saturated porous materials using a flexible wall permeameter. ASTM International.

ASTM D., 2011. Standard test method for direct shear test of soils under consolidated drained conditions, 9p.

Bhardwaj A., Shainberg I., Goldstein D., Warrington D., J. Levy G., 2007. Water retention and hydraulic conductivity of cross-linked polyacrylamides in sandy soils. Soil Science Society of America Journal, 71(2), 406-412.

Bouazza A., Gates W.P., Ranjith P.G., 2009. Hydraulic conductivity of biopolymer-treated silty sand. Géotechnique, 59(1), 71-72.

Chang I., Cho G.-C., 2019. Shear strength behavior and parameters of microbial gellan gum-treated soils: from sand to clay. Acta Geotechnica, 14(2), 361-375.

Chang I., Im J., Cho G.-C., 2016. Geotechnical engineering behaviors of gellan gum biopolymer treated sand. Canadian Geotechnical Journal, 53(10), 1658-1670.

Chang I., Im J., Prasidhi A.K., Cho G.-C., 2015a. Effects of Xanthan gum biopolymer on soil strengthening. Construction and Building Materials, 74, 65-72.

Chang I., Prasidhi A.K., Im J., Shin H.-D., Cho G.-C., 2015c. Soil treatment using microbial biopolymers for anti-desertification purposes. Geoderma, 253, 39-47.

El-Rehim H.A., Hegazy E.S.A., El-Mohdy H.A., 2004. Radiation synthesis of hydrogels to enhance sandy soils water retention and increase plant performance. Journal of Applied Polymer Science, 93(3), 1360-1371.

Fell R., 2005. Geotechnical engineering of dams. CRC press.

Fredlund D., Morgenstern N.R., Widger R., 1978. The shear strength of unsaturated soils. Canadian Geotechnical Journal, 15(3), 313-321.

Fredlund D.G., Rahardjo H., Fredlund M.D., 2012. Unsaturated soil mechanics in engineering practice. John Wiley & Sons.

Hatakeyama H., Hatakeyama T., 1998. Interaction between water and hydrophilic polymers. Thermochimica Acta, 308(1-2), 3-22.

Hendriks C.A., Worrell E., De Jager D., Blok K., Riemer P., 1998. Emission reduction of greenhouse gases from the cement industry. In Proceedings of the fourth international conference on greenhouse gas control technologies. IEA GHG R&D Programme Interlaken, Austria, 939-944.

ITASCA, 2011. Fast Lagrangian Analysis of Continua, Version 7.0, Itasca Consulting Group.

Jeong S., Kim Y., Lee J.K., Kim J., 2015. The 27 July 2011 debris flows at Umyeonsan, Seoul, Korea. Landslides, 12(4), 799-813.

Ko D., Kang J., 2020. Biopolymer-reinforced levee for breach development retardation and enhanced erosion control. Water, 12(4), 1070.

Mayer L., Silva W.P.D., Moura A.B., Vendruscolo C.T., 2010. AFLP analysis of Xanthomonas axonopodis and X. arboricola strains used in Xanthan production studies reveal high levels of polymorphism. Brazilian Journal of Microbiology, 41, 741-748.

Mualem Y., 1976a. A new model for predicting the hydraulic conductivity of unsaturated porous media. Water Resources Research, 12(3), 513-522.

Mualem Y., 1976b. Hysteretical models for prediction of the hydraulic conductivity of unsaturated porous media. Water Resources Research, 12(6), 1248-1254.

Osacky M., Geramian M., Ivey D.G., Liu Q., Etsell T.H., 2015. Influence of nonswelling clay minerals (illite, kaolinite, and chlorite) on nonaqueous solvent extraction of bitumen. Energy & Fuels, 29(7), 4150-4159.

Palaniraj A., Jayaraman V., 2011. Production, recovery and applications of xanthan gum by Xanthomonas campestris. Journal of Food Engineering, 106(1), 1-12.

Seki K., 2007. SWRC fit a nonlinear fitting program with a water retention curve for soils having unimodal and bimodal pore structure. Hydrology and Earth System Sciences Discussions, 4(1), 407-437.

Tran A.T.P., Chang I., Cho G.-C., 2019. Soil water retention and vegetation survivability improvement using microbial biopolymers in drylands. Geomechanics and Engineering, 17(5), 475-483.

Tran T.P.A., Cho G.-C., Chang I., 2020. Water retention characteristics of biopolymer hydrogel containing sandy soils. Hue University Journal of Science: Earth Science and Environment, 129(4A), 5-17.

Van Genuchten M.T., 1980. A closed-form equation for predicting the hydraulic conductivity of unsaturated soils. Soil Science Society of America Journal, 44(5), 892-898.

Wang S., Zhao X., Zhang J., Jiang T., Wang S., Zhao J., Meng Z., 2023. Water retention characteristics and vegetation growth of biopolymer-treated silt soils. Soil and Tillage Research, 225, 105544. https://doi.org/10.1016/j.still.2022.105544.

Wang Z., Wu L., Wu Q.J., 2000. Water-entry value as an alternative indicator of soil water-repellency and wettability. Journal of Hydrology, 231, 76-83.

Yang H., Rahardjo H., Leong E.-C., Fredlund D.G., 2004. Factors affecting drying and wetting soil-water characteristic curves of sandy soils. Canadian Geotechnical Journal, 41(5), 908-920.

Zhang H., Fang B., Lu Y., Qiu X., Jin H., Liu Y., Wang L., Tian M., Li K., 2017. Rheological properties of water-soluble cross-linked xanthan gum. Journal of Dispersion Science and Technology, 38(3), 361-366.

Zhang J., Meng Z., Jiang T., Wang S., Zhao J., Zhao X., 2022. Experimental Study on the Shear Strength of Silt Treated by Xanthan Gum during the Wetting Process. Applied Sciences, 12(12), 6053. https://doi.org/10.3390/app12126053.